EXPERIMENTAL INVESTIGATION OF GSM 900 MHz RESULTS OVER NORTHERN INDIA WITH AWAS ELECTROMAGNETIC CODE AND OTHER PREDICTION MODELS

M. V. S. N. Prasad[1,*], P. K. Dalela[2], and C. S. Misra[3]

[1]CSIR-National Physical Laboratory, Dr. K S Krishnan Road, New Delhi 110012, India

[2]C-DOT, Mandigaon Road, Opp. New Manglapuri, Chatterpur, Mehrauli, New Delhi 110030, India

[3]Aircom International Pvt Ltd., Gurgaon 122001, India

Abstract—Recent trends in propagation modeling indicate the study of mobile radio propagation modeling with the help of electromagnetic formulations which traditionally has been explained with empirical methods. These empirical methods were preferred by the cellular operators in their radio planning tools due to their ease of implementation and less time consumption. In the present study, AWAS electromagnetic code and conventional prediction methods have been employed to explain the observed results of ten base stations mainly in the near field zones of GSM 900 MHz band situated in the urban and suburban regions around Delhi in India. The suitability of the above models in terms of prediction errors and standard deviations are presented. Path loss exponents deduced from the observed data have been explained by Sommerfeld's formulations.

1. INTRODUCTION

In order to design high quality and high capacity cellular networks, a thorough understanding of propagation channel is necessary, and signal strength measurements should be conducted to delineate cell radii and assess reliable coverage area [1]. It is established that propagation phenomena can cause unexpectedly poor performance in cellular networks. These are manifested in reduced coverage,

dropped calls and unexpected hand overs [2]. The performance of the cellular network can be assessed, or new networks can be designed when different models are tested with observed results. Arijit De et al. pointed out [3] that in cellular communication scenario not much attention is paid to the relationship between the height of the transmitting antenna and the distance of transition from near field to far field region. In the near field, the strength of the field oscillates wildly with large nulls and peaks. They indicated that larger was the height of transmitting antenna, greater would be the near field region, and the performance of cellular communication systems was degraded appreciably in near field region rather than in the far field region. They positioned the antenna closer to ground and also deployed a horizontally polarized antenna for mobile communications as the fields radiated by a horizontally polarized antenna not to vary too much with the height of the antenna in the near field region. Gutierrez-Meana et al. [4] used deterministic radio electric coverage tool for the computation of electromagnetic fields based on modified equivalent current approximation method. They illustrated the applicability in a rural scenario, where a GSM base station at 900 MHz is located, and an urban scenario to test the acceleration technique.

Most of the statistical propagation models used in radio planning tools for the design of cellular radio networks refer to the period of GSM where antennas are located far above the roof top, and cells were large [5]. Latest developments in mobile radio technology and introduction of smaller cells, lower antennas necessitated the development of models applicable to many situations. The special feature in Delhi urban environment is that most of the buildings are non uniformly spaced, and results reported elsewhere might not be totally applicable to this type of environment. In this context, it is worthwhile to investigate how numerical electromagnetic codes compete with the statistical propagation models in the 900 MHz band. Prasad et al. reported the investigation of eleven base station results in the 1800 MHz band with AWAS code and other models [6]. To verify the suitability of AWAS electromagnetic code in the 900 MHz band, field strength measurements were conducted utilizing the following GSM base stations situated in national capital region of Delhi. They are 1. Paschimvihar (PVR) 2. University Area (UA) 3. Nandanagari-1 (NN-1). 4. Nandanagari-2 (NN-2) 5. Satyaniketan (SNT) 6. Faridabad (FBD) 7. Vinayak Hospital (VKH) in the urban region and three suburban base stations namely 1. Tradex tower (TXT), 2. Meethapur (MTR) 3. Gurgaon (GRN). The measured values of signal strength have been compared with the prediction methods of AWAS, Hata, COST 231 Walfisch & Ikegami, Dmitry and ITU-R. The models have

been chosen so that they are applicable to the environments where measurements were conducted.

2. ENVIRONMENTAL DESCRIPTIONS

1. Both the NN-1 and NN-2 base stations are surrounded by dense urban areas on three sides and medium urban environment on the other side. The average building height is around 6 to 9 m. PVR base station is surrounded by medium urban environment with slight open areas in between. Far away from the base station on the left side, low tree density is seen. On the southern side of the base station, a small water canal flows. UA base station is surrounded by medium urban environment, and from east to south of the base station, a thick patch of tree density is seen. At a distance 2 km away from the base station, dense urban environment prevails on the southern side of the base station.

(a)

(b)

(c)

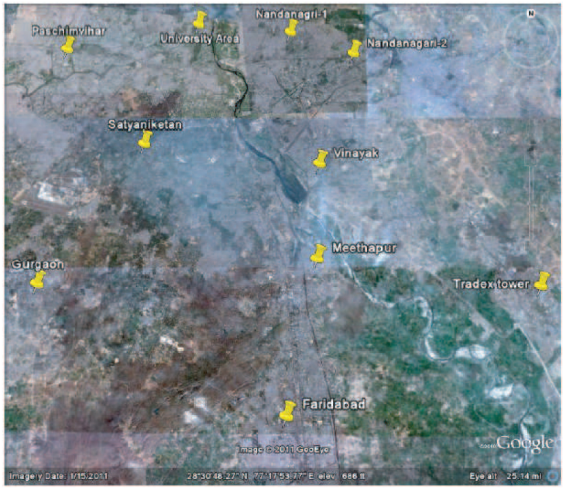

(d)

Figure 1. (a) Photographs of the environment. (b) Photographs of the environment. (c) Photographs of the environment. (d) Google map showing the locations of base stations.

MPR base station is surrounded by low density urban area (mainly suburban) with small patches of green vegetation in between. SNT base station is surrounded by medium urban environment and small patches of greenery in between, denoting some kind of low urban residential environment. Figures 1(a) to 1(c) show the photographs of the environment where measurements were conducted. A google map showing the locations of 10 base stations is shown in Figure 1(d). The three photographs in Figures 1(a) to 1(c) were taken from the close surrounding area of base stations VKH, FBD and SNT. Since the environmental features of other base stations are more or less similar, they are described in detail.

3. EXPERIMENTAL DETAILS

The transmitting power of all base stations is 43.8 dBm, and transmitting gain is 2 dBi for all base stations except GRN base station where it is 8 dBi. The gain of the receiving antenna is 0 dB and the height 1.5 m. The height of the base station above the ground level and co-ordinates of the base stations are shown in Table 1. The receiver is standard Nokia equipment used in drive in tools for field trials. The position of the mobile is determined from the GPS receiver, and this information with the co-ordinates of the base station was utilized to deduce the distance traveled by the mobile from the base station. The signal strength information recorded in dBm was converted into path loss values utilizing the gains of the antenna. The data were recorded with 512 samples in one second on a laptop, and the number of samples collected for each site varied from 1×10^5 to 2×10^5. Measured r.m.s. error is around 1.5 dB. Data were averaged over conventional figure of 40λ.

4. PREDICTION METHODS

The following prediction methods have been utilized in this study. 1. AWAS numerical code based on electromagnetic modeling [7].

Table 1. Details of base stations used in the study.

Urban region	h_b (m)	Lat (deg)	Long (deg)	Maximum Near field Distance (m)
PVR	13	28.6738	77.08882	236
UA	24	28.69655	77.21367	436
NN-1	14	28.66912	77.36256	220
NN-2	12	28.68908	77.3026	189
SNT	18	28.58845	77.16848	284
FBD	10	28.38071	77.29720	158
VKH	13	28.57132	77.32809	205
Suburban region				
TXT	43	28.47266	77.51447	678
MTR	12	28.49434	77.32450	189
GRN	20	28.4753	77.08445	315
	$hm = 1.5$			

2. ITU-R method [8]. 3. Dmitry model [9]. 4. COST 231 Walfisch-Ikegami method [10]. 5. Hata method [11].

4.1. AWAS Numerical Electromagnetic Code

AWAS electromagnetic code has been utilized to compare the predictions in the near field and far field zones. It is utilized to compute the path loss values with different values of dielectric constant and conductivity of 2×10^{-4} over real ground. The commercially available computer program is capable of analyzing wire antennas operating in transmitting and receiving modes as well as analyzing wire scatterers. Different values of dielectric constant for dense urban, urban and suburban regions have been incorporated in the computation of AWAS simulation. Reference [12] gives dielectric constants for various types of grounds and environments. It gives values of 3–5 for city industrial area. Hence a value of 4 is used in the simulation of AWAS for dense urban base stations. The same reference gives a value of 10 for fertile lands and a value of 15 for agricultural lands. In the present study there is no region of fertile land and agricultural lands, but urban and suburban regions. In this study, the type of ground is the same in the case of all base stations, and the difference in urban and suburban regions comes from the degree of urbanization. In [13], a value of 4 for dielectric constant has been chosen for urban region when real earth is considered with imperfectly conducting ground. Keeping these aspects in view, we have carefully chosen a value of 6 for urban base stations and a value of 8 for suburban base stations in the AWAS simulation. The technique is based on the two-potential equation for the distribution of wire currents. This integro–differential equation is solved numerically using the method of moments with a polynomial approximation for the current distribution. The influence of ground is taken into account using Sommerfeld's approach with numerical integration algorithms developed exclusively for this program. The program evaluates the fields in the near and far field regions, and the fields were converted into path losses to compare with the observed values.

4.2. ITU-R Model

ITU-R recommendation 1411-4 provides prediction capability for outdoor short range radio communication systems and radio local area networks in the frequency range 300 MHz–100 GHz and gives closed-form algorithms both for site-specific and site-general calculations. The model is applicable to urban high rise, low rise urban, suburban, residential and rural areas. In the case of dense urban or urban under

nlos (non line-of-sight) category the range of applicability of this model is, base station antenna height (h_b) from 4 to 50 m, mobile antenna height (h_m) from 1 to 3 m, frequency (f) from 800 to 5000 MHz, and 2 to 16 GHz for $h_b < h_m$ and distance (d) from 20 to 5000 m. In the case of suburban regions, any height of h_m can be used, $\Delta\ h_b$ from 1 to 100 m ($\Delta\ h_b$ is the difference of base station and average roof heights), $\Delta\ h_m$ from 4 to 10 m ($\Delta\ h_m$ is the difference of roof height and mobile heights), street width (w) ranging from 10 to 25 m and d from 10 to 5000 m. Multiscreen diffraction terms are incorporated to account the roof top diffractions in the urban zone. Here the average roof top height is used. In the nlos category for roof tops of similar height, the loss is expressed as sum of free space loss, multiscreen diffraction loss and loss due to coupling of wave propagation along the multiscreen path into the street where mobile is located. Here width of the street is taken into consideration. For more details the reader can refer to ITU-R recommendation. In the case of suburban zones propagation model based on geometrical optics is given.

4.3. Dmitry Model

Dmitry method comes under stochastic category. In the case of Dmitry method, propagation modeling is done by explicitly considering random diffuse scattering at street level in the vicinity of the mobile and propagation over clutter as a deterministic problem. The authors compare their model over an urban environment with COST 231 Hata, Walfisch-Bertoni models at 2 GHz, for base station antenna height of 25 m, clutter height of 20 m and street width of 30 m and mobile antenna height of 2 m. In another study Yarkoni et al. [14] investigated the total received signal for mobile antenna in urban region based on multi parametric stochastic approach. They claimed that their equations can predict different propagation situations and path loss in various urban channels for different heights of base station and mobile terminal antennas.

4.4. Walfisch-Ikegami (WI) Method

Walfisch-Ikegami (WI) method is one of the most widely used analytical models to predict the path loss which consists of a combination of Walfisch and Ikegami models. Here the path loss is a combination of free space loss, multiple knife-edge diffraction to the top of the final building and single diffraction and scattering process down to street level. The model is applicable to frequencies between 800 to 2000 MHz; h_b between 4 and 50 m, h_m between 1 and 3 m, and distances between 200 to 5000 m. Performance of the model is poor

when h_b is less than h_m. In the present study, this model is utilized for street width of 20 m and roof heights of 12 and 15 m.

4.5. Hata Method

The well-known Hata model is a fully empirical model based entirely upon extensive series of measurements made in Tokyo City between 200 MHz and 2 GHz [11]. Different equations are available for urban, suburban and open zones.

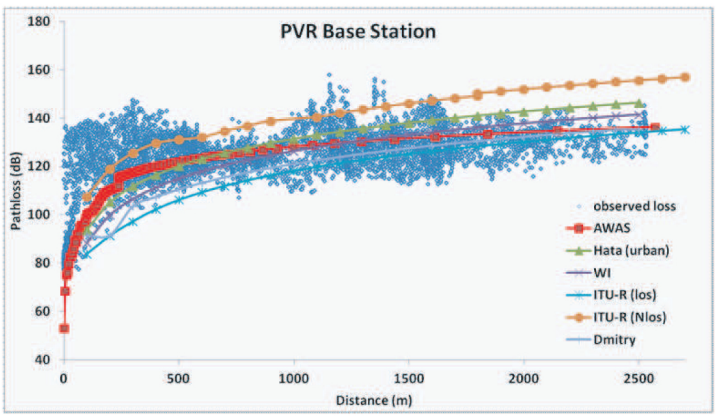

Figure 2. Comparison of observed path loss values with various models for PVR base station.

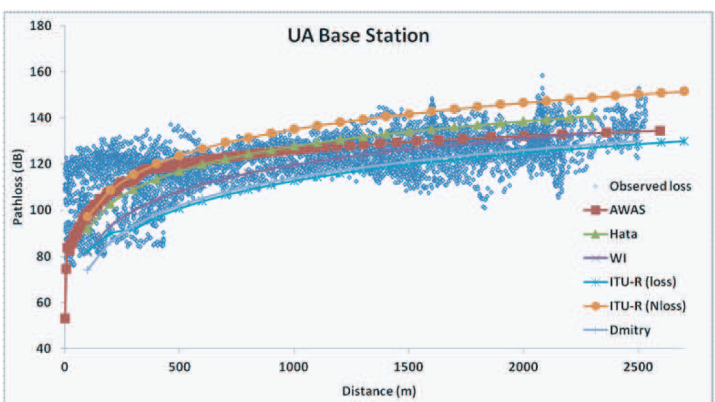

Figure 3. Comparison of observed path loss values with various models for UA base station.

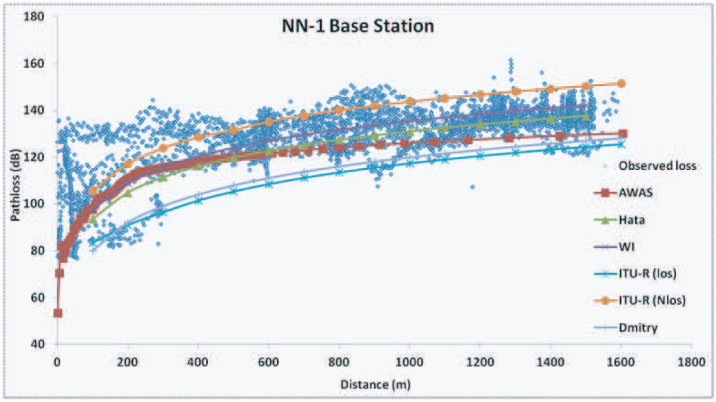

Figure 4. Comparison of observed path loss values with various models for NN-1 base station.

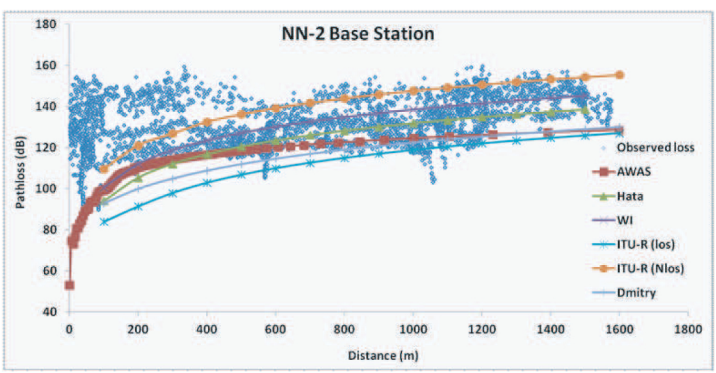

Figure 5. Comparison of observed path loss values with various models for NN-2 base station.

5. RESULTS

The comparison of the above prediction methods with observed values of path loss for base stations PVR, UA, NN-1, NN-2, SNT, FBD,VKH, TXT, MTR and GRN base stations are shown in Figures 2–11. The ending of the near field distances designated as near field maximum computed for all the base stations are shown in Table 1. The maximum near field distance has been computed using the formula $4h_b\ h_m/\lambda$ taken from the extensive discussion on near and far field effects on cellular communication systems from the work of Arijit De et al. [3].

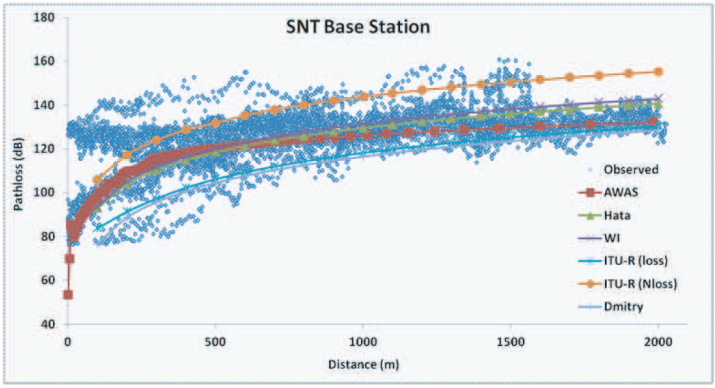

Figure 6. Comparison of observed path loss values with various models for SNT base station.

The variations in the near field are more important than in the far field since the observed path loss of cellular communication system in near field region shows large variations. In Figure 2, close to the transmitter below 500 m, the observed values of path loss vary between 80 to 140 dB, showing large dispersion of path loss values, and beyond 500 m, are confined between 100 and 150 dB. Beyond 500 m, the path loss has less dispersion. AWAS numerical code and Hata method for urban regions show good agreement with the observed values. ITU-R (nlos) overestimates the observed values beyond 500 m. Path loss curves of Dmitry and WI methods pass through the lower part of the observed path loss values. ITU-R (los) method appreciably underestimates especially in the region below 1000 m. In Figure 3 for UA base station observed values below 500 m vary between 80 to 130 dB, and large dispersion of path loss is seen in this region. Beyond 500 m, path loss is confined between 90 and 135 dB up to 2500 m. Similar to Figure 2, AWAS and Hata methods give good agreement. Predicted path loss graphs of Dmitry and WI methods pass through the lower half of the observed path loss patch; ITU-R (los) passes through the lower part of observed loss; ITU-R (nlos) passes through the upper region of observed loss. At a given distance, the observed loss varies approximately by 20 dB. In fact, both the curves can be used to predict the variability of path loss. More or less similar trend is seen for the remaining Figures 4 to 11 for the other base stations. Some interesting features observed in these figures are described below.

In Figures 4 & 5 for NN-1 and NN-2 base stations, observed loss below 500 m is moderately higher than those in Figures 2 and 3 due to very narrow street widths and congested urban settings (buildings

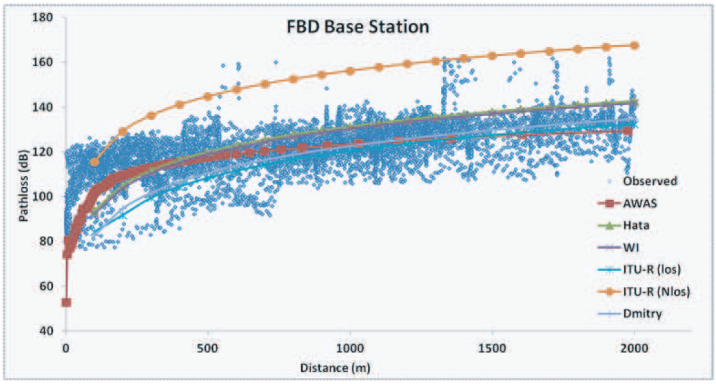

Figure 7. Comparison of observed path loss values with various models for FBD base station.

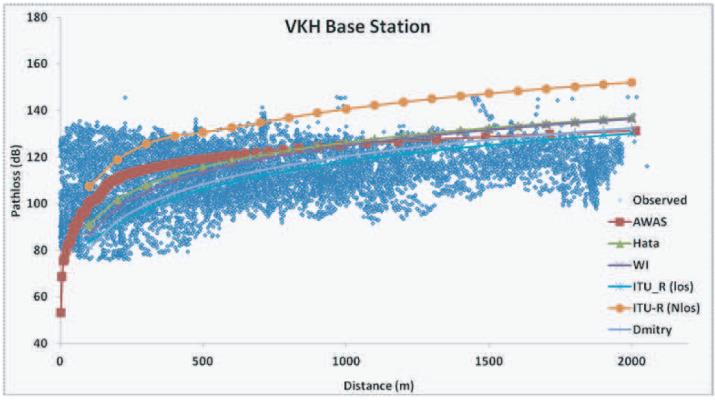

Figure 8. Comparison of observed path loss values with various models for VKH base station.

are non uniform also). Hence AWAS and Hata methods appear to pass through the lower half of observed path loss patch. ITU-R (los) and Dmitry methods underestimate by 20 to 25 dB. In Figure 5, the observed losses below 200 m are higher than that of Figure 4 probably due to the location of base station in zones where street widths are narrower than that of Figure 4's base station. In Figures 6 & 7, for SNT and FBD base stations variation of observed path loss is similar to Figs. 2 & 3. Observed path loss varies between 80 to 120 dB below 500 m and beyond this varies between 90 to 140 dB. Prediction methods AWAS,

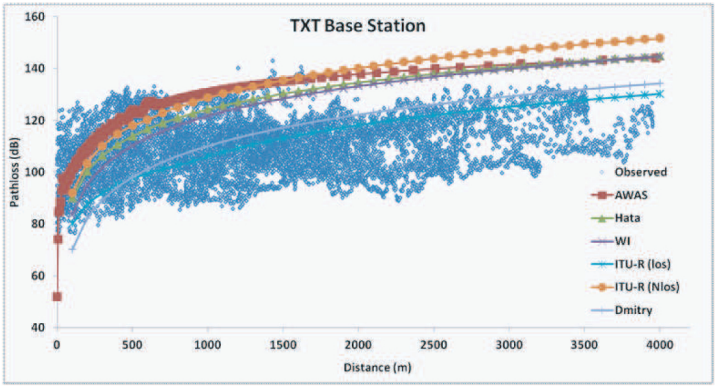

Figure 9. Comparison of observed path loss values with various models for TXT base station.

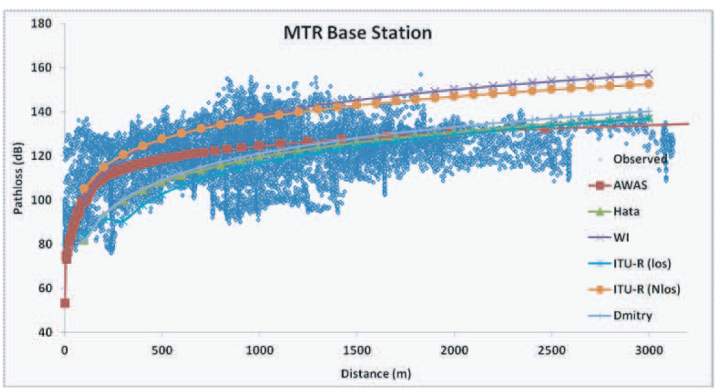

Figure 10. Comparison of observed path loss values with various models for MTR base station.

Hata and WI give good agreement with the observed loss whereas that of Dmitry and ITU-R(los) pass through the lower side of observed path loss patch. ITU-R (nlos) method overestimates appreciably. Lower observed path loss values are probably due to wider street width and more or less uniform structure of buildings yielding less losses than those of Figures 4 & 5. Figure 8 exhibits variations similar to Figure 7 due to similarities in urban structure.

In the case of Figure 9, the observed path loss varies between 80 to 120 dB below 500 m and beyond that 90 to 120 dB up to 4000 m. Beyond break point path loss getting confined to a range of values

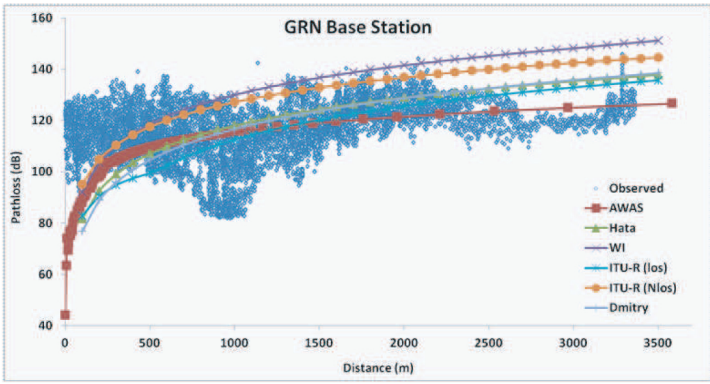

Figure 11. Comparison of observed path loss values with various models for GRN base station.

is due to the less variations of signal in far field region and large dispersion of path loss in the near field region. Figures 10 & 11 show a similar trend with reference to the prediction methods discussed above. Overall in the near field region, path loss varies by as much as 50 to 60 dB where as in the far field region the variations get reduced to 20 to 25 dB, and it is for this reason that most of the prediction methods do not give good agreement in the near field region compared with the far field region. In Figure 10, AWAS, Hata, Dmitry show good agreement, and ITU-R (nlos) method shows good agreement till 2000 m and beyond that overestimates. ITU-R (los) curve passes through the lower patch of observed loss and moderately agrees. Figure 11 also exhibits a similar trend.

Explanation of the deviations: The difference in path loss calculated from AWAS electromagnetic code and measurement could be due to the different values of excitations chosen in the measurement and in the analysis of transmitting antenna. For the measurement, the transmitting antenna had a high gain, whereas in the numerical computation, we considered a simple dipole centrally excited by one volt. However, the curve due to AWAS passes through the thick cluster of observed values. Sarkar et al. [13] have shown that even in urban environment numerical electromagnetic codes based on Sommerfeld theory derived from Maxwell's postulates can be used to predict propagation characteristics. If one knows the electrical characteristics of the earth, it is possible to predict how the field strength will vary with the distance without carrying the experimental measurements. Ray tracing is more suitable for far field predictions than near field predictions.

6. STANDARD DEVIATIONS OF THE PREDICTION METHODS

Based on the above comparison, prediction errors of the models have been deduced where prediction error is given by the difference of the observed and predicted values. Standard deviations of all the base stations for the above methods have been calculated and are shown in Table 2. In the table, ME refers to mean error and SD to standard deviation. In the case of AWAS the lowest standard deviation of 8.1 is seen for PVR base station and the highest value of 23.2 for NN-2 base station. The average value of standard deviation for all urban base stations is 12.78 and for suburban stations is 13.6. In the case of

Table 2. Standard deviations and mean errors (in dB) of the prediction methods.

Base station	AWAS		Hata		WI	
	ME	SD	ME	SD	ME	SD
PVR	0.3	8.1	−2.5	11.0	0.8	11.0
UA	−1.8	9.5	−3.4	10.5	2.0	10.6
NN-1	5.0	9.7	3.5	10.4	0.6	10.2
NN-2	7.5	23.2	7.3	13.8	2.4	12.8
SNT	2.2	12.3	0.5	12.9	−0.7	13.0
FBD	−1.4	12.2	−5.6	13.2	−4.8	12.5
VKH	−6.3	14.5	−9.2	21.6	−6.0	16.0
TXT	−19.1	16.3	−16.0	16.8	−14.5	17.2
MTR	−2.4	12.8	−0.2	14.3	−14.9	17.5
GRN	0.5	11.7	−2.9	14.3	−13.8	16.7
Base station	ITU-R(los)		ITU-R(nlos)		Dmitry	
	ME	SD	ME	SD	ME	SD
PVR	6.8	12.3	−11.3	12.3	4.3	10.8
UA	6.3	10.8	−9.8	12.3	5.9	11.4
NN-1	15.6	13.4	−4.8	10.8	14.0	13.3
NN-2	21.2	16.1	−3.6	12.8	15.9	14.7
SNT	8.0	14.1	−9.7	14.9	9.3	14.8
FBD	−22.0	20.3	-32.3	16.4	0.3	12.8
VKH	−1.0	14.9	−21.5	18.4	−2.4	15.4
TXT	−3.1	16.3	−20.5	18.3	−4.3	15.2
MTR	1.3	14.7	−13.5	16.4	−1.5	15.3
GRN	0.17	14.1	−9.8	14.7	−2.3	15.0

Hata method, the lowest value of 10.5 for UA base station and 10.4 for NN-1 base station and highest value of 21.6 for VKH base station are observed. The average value of standard deviation for all urban base stations is 13.34 and for suburban stations is 15.13. WI also follows a similar trend, and the average value of standard deviation for all the urban base stations is 12.13 and for suburban base stations is 17.13. In the case of ITU-R (los), average value for urban base stations is 14.55 and for suburban base stations is 15.03. For ITU-R (nlos) and Dmitry, the corresponding values are 13.98 and 13.31 for urban base stations and 16.46 and 15.16 for suburban base stations, respectively. From the above discussion, it appears that AWAS numerical code has a slight edge over others followed by Hata and WI methods.

7. PATHLOSS EXPONENTS

The observed values of path loss for all the base stations have been deduced for distances ranging from 50 m to 3.5 km. Path loss exponents from the data have been computed from Equation (1) shown below using the observed path losses for various distances

$$L = L_0 + 10n \log d + S \tag{1}$$

where L is the path loss deduced for various distances, L_0 the path loss at one meter, d the distance in meters, and S the shadow fading in dB. Using the approach given in [15] of Erceg et al., the path loss exponent n has been deduced. In the above equation

$$L_0 = 20 \log(4\Pi d_0/\lambda) \tag{2}$$

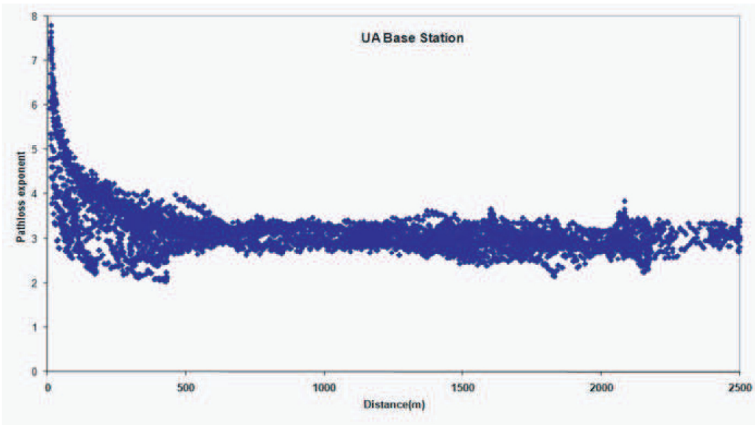

Figure 12. Path loss exponent as a function of distance for UA base station.

where λ is the wavelength corresponding to 900 MHz, and d_0 is taken as one meter. S is the shadow fading variation, varies from location to another within given macrocell, and tends to be Gaussian in a given macro cell denoting shadow fading as lognormal. It can be expressed as $s = y\sigma$, where y is a zero mean Gaussian variable of unit standard deviation, and σ the standard deviation of S is itself a Gaussian variable over macrocells. L is taken from the observed path loss values. Using the above values, the path loss exponent 'n' has been deduced and shown in Figures 12–15 for some base stations UA, SNT, FBD and VKH. In all these diagrams, the exponent close to transmitter exhibits higher values of the order of 8, falls steeply and stabilizes to a value of around 3, and remains the same for the rest of the distances denoting stable values in the far field zone. These figures have great significance in delineating near and far field regions from the observed data and can serve as design inputs for fixing the boundaries of cell radii. Closer is the transition point of near field to far field zone to the transmitter, better will be the performance of cellular communication network.

It is well known that in the near field regions the path loss exponent is 3 due to the static nature of the fields. The path loss exponent should be around 6 as there is no static nature in it. Figures 12–15 showing the variation of path loss exponent as a function of distance depict high path loss exponent values at distances close to transmitter, and they fall steeply till the end of near field zone. Beyond these values, the exponent remains more or less stable. In the path loss

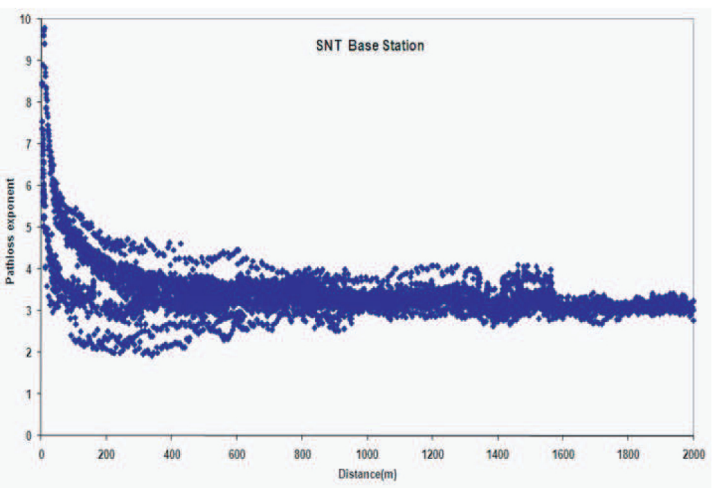

Figure 13. Path loss exponent as a function of distance for SNT base station.

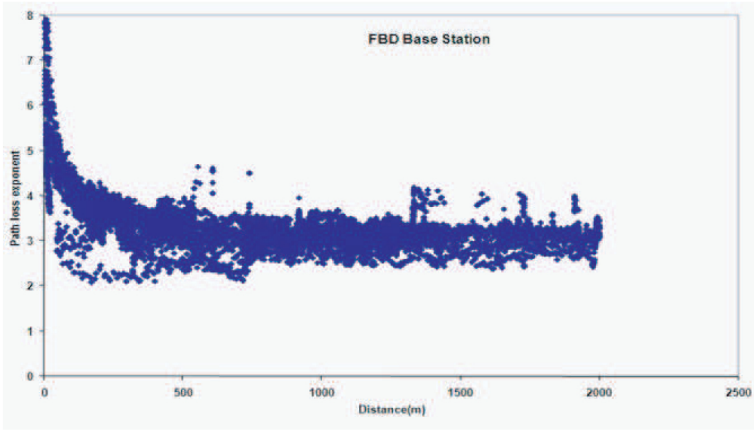

Figure 14. Path loss exponent as a function of distance for FBD base station.

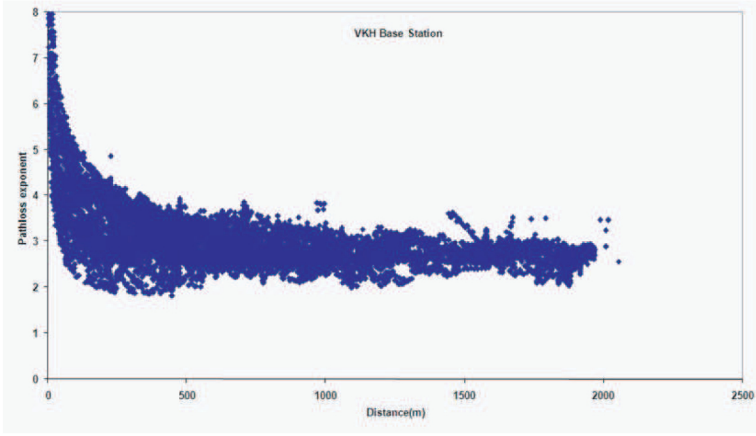

Figure 15. Path loss exponent as a function of distance for VKH base station.

exponent diagrams (Figures 12–15), the curve turns at an exponent of 4 and stabilizes with a value of 3 for the remaining distances called intermediate distances. Sarkar [16] through accurate numerical analysis using Sommerfeld formulations showed that at distances very far away from the base station (beyond intermediate distances), the exponent starts increasing to a value of 4. Figures 12–15 depict up to intermediate distances where the exponent gets stabilized to a value of 3, in accordance with the Sommerfeld's propositions. In other words, the present data substantiated many of the Sommerfeld's findings, and physics based macro modeling would be sufficient to explain many of

the observed results.

Sarkar et al. [13] have shown that when antenna is placed on the top of a cellular tower, it produces highly undesirable radiation pattern. Moreover, the signal strength goes through a series of maxima and minima even though the antenna is located and radiating in free space.

This type of radiation pattern for a dipole transmitting antenna is natural due to interference between the fields from the original dipole with its image created by the presence of ground and not due to the buildings as no building parameters are present in AWAS. If the antenna is located at 100 m or above as in a microwave line-of-sight link, lobing effects in the pattern will be minimized as the strength of image will be reduced due to losses in the ground. Sommerfeld's theory predicts that the effects of surface wave will be minimal as one goes away from the antenna and that the interference between the space wave and surface wave will be less reducing the lobing effects in the pattern. This has been exhibited by the above discussed path loss exponent diagrams with variations coming strongly in the near field region due to the antenna heights situated between 20–30 m.

8. BREAK POINT DISTANCES

The break point has been deduced as the distance at which the slope of the curve (the path loss exponent vs distance) changes. In Figure 12, it changes at 300 m. Observed break point has been taken from the diagrams showing the variation of path loss exponent as a function of distance and shown in Table 3. An examination of these path loss exponent curves shows that at distances close to transmitter, exponent falls rapidly from higher values, and the slope of the curve changes at

Table 3. Break point distances observed from data.

Base station	Height of tx. ant (m)	Observed break point (m)
1. PVR	13	300
2. UA	24	300
3. NN-1	14	200
4. NN-2	12	200
5. SNT	18	300
6. FBD	10	300
7. VKH	13	300
8. TXT	43	400
9. MTR	12	250
10. GRN	20	500

a particular distance. We have reported these distances at which the slope of the curve changes as the break point for various base stations. The end of the near field or maximum near field distance represents the end of the region where rapid variations of signal are seen. Beyond the maximum near field distance, far field region starts where the path loss exponent is more or less stabilized. In the far field region, only height gain of antenna is seen.

Examination of the above table shows that the position of the break point distance depends not only on the height of the base station antenna, but also on the type of terrain and environment surrounding the base station. In the case of suburban base stations for the same antenna height, the break point is larger than the corresponding stations in the urban zone. For example, in the case of SNT base station with antenna height of 18 m, the break point is found at 300 m whereas in the suburban region base station GRN with antenna height of 20 m, the break point is found at 500 m. In urban environment, the break point is seen at smaller distances which could be due to high density of urbanization.

Discussion: In the case of [15] by Erceg et al., who made extensive measurements at 1.9 GHz at New Jersey, Seattle and Chicago, high path losses close to the transmitter were observed, and then the loss decreased linearly with distance. In the present study, the path loss is falling steeply up to 0.5 km. The nature of variation of path loss exponent in the present study resembled the variation in Erceg et al.'s study. Steep transitions of path loss occur when the base station antenna height is close to the height of surrounding building roof tops. Hence the height accuracy of the base station antenna is especially significant if large prediction errors are to be avoided [17]. Milanovic et al. [18] have observed that in dense urban regions measurements show a very interesting feature. Path loss after the break point does not increase with distance, probably due to the wave guiding effect of city streets as well as the existence of radio wave components reflected and diffracted on buildings reaching the receiver antenna. The path loss exponent in the present study showed this trend. Herring et al. [19] observed a large variance in received power as a function of distance. This showed that using a single value of path loss exponent for a particular neighbourhood as assumed in popular empirical models can lead to large errors in path loss estimates. High path losses close to the transmitter require higher margins from operators. The deviation of all the prediction methods at closer distances to the transmitter is high due to the large path loss variation.

Another advantage of studying path loss exponent as a function of distance is the identification of exclusion zones. These are the

zones around base stations within which emf's exposure guide lines are exceeded in order to protect the general public from potential harmful levels of radiation [20]. In the reactive near field, radiative near and far field regions around base station, radiated field does not present the same behavior, and adequate propagation models are required to estimate the exact field strength at any specific distance. Typically, exclusion zones around base station antennas, inside which exposure thresholds may be exceeded, are in the near field zone of radiating antenna (some meters).

Baltzis [21] showed that path loss cumulative distribution function was dependent on path loss exponent and system geometry. Effect of wet forest on the deployment of Zigbee network has been investigated by Gay-Fernandez et al. [22], and Helhel et al. [23] investigated dry and wet earth effects on GSM 900&1800 MHz propagation in Turkey. Phaiboon and Phokharatkul [24] using modified Xia model investigated 900&1800 MHz measurements. Pu et al. [25] estimated small scale fading characteristics of RF wireless link under railway communication environment. For next generation wide band communication systems spectrum efficiency could be increased, and signal quality could be improved with the implementation of co-ordination scheme among base stations [26]. Three dimensional ray tracing methods in urban microcellular environments have been utilized by Liu and Guo [27].

9. CONCLUSIONS

In the present study, the observed path losses from 10 base stations operating in the GSM 900 MHz band situated in the urban and suburban regions of Delhi have been compared with the AWAS electromagnetic code and conventional prediction methods, such as Hata, WI, Dmitry and ITU-R. Overall AWAS, Hata & WI curves show good agreement with the observed values. These curves pass through the centre of the observed cluster of path losses. In the near field region, AWAS predicts the observed values better than Hata & WI methods. In the suburban/low density urban regions, ITU-R (nlos) curve overestimates path losses by 20 dB. The average values of standard deviations reported by AWAS are 12.78 and 13.6 for urban and suburban base stations with Hata showing 13.34 and 15.13 and WI 12.13 and 17.13, respectively. AWAS numerical code has shown more or less the same deviation in urban and suburban regions, is suitable for any type of environment, and does not require any tuning of the coefficients unlike other methods. The difference in standard deviations for other methods ranges from 3–5 dB for urban and suburban regions. From the observed path losses values, path loss exponents as a function

of distance have been calculated, and from these curves break point distances have been deduced. These have been explained in terms of transitions between near and far field zones. Higher path losses observed in the near field zones of base stations require novel strategies to improve the performance of cellular networks.

REFERENCES

1. Nadir, Z. and M. I. Ahmad, "Pathloss determination using Okumara-Hata model and cubic regression for missing data for Oman," *Proc. of the International Multi Conference of Engineers and Computer Scientists, IMECS 2010*, Vol. 11, 804–807, Hong Kong, Mar. 17–19, 2010.
2. Kwakkernaat, M. R. J. A. E. and M. H. A. J. Herben, "Diagnostic analysis of radio propagation in UMTS networks using high resolution angle-of-arrival measurements," *IEEE Antennas and Propagation Magazine*, Vol. 53, No. 1, 66–75, Feb. 2011.
3. De, A., T. K. Sarkar, and M. Salazar-Palma, "Characterization of the far field environment of antennas located over a ground plane and implications for cellular communication systems," *IEEE Antennas and Propagation Magazine*, Vol. 52, No. 6, 19–40, Dec. 2010.
4. Gutierrez-Meana, J., J. A. Martinez-Lorenzo, F. Las-Heras, and C. Rappaport, "DIRECT: A deterministic radio coverage tool," *IEEE Antennas and Propagation Magazine*, Vol. 53, No. 2, 135–145, Apr. 2011.
5. Mantel, O. C., J. C. Oosteveen, and M. P. Popova, "Applicability of deterministic propagation models for mobile operators," *Second European Conf. on Antennas and Propagation, Eucap 2007*, 11–16, Nov. 2007, Print ISBN. 978-0-86341-842-6.
6. Prasad, M. V. S. N., S. Gupta, and M. M. Gupta, "Comparison of 1.8 GHz cellular outdoor measurements with AWAS electromagnetic code and conventional models over urban and suburban regions of northern India," *IEEE Antenna and Propagation Magazine*, Vol. 53, No. 4, 76–85, Aug. 2011.
7. Djordjevic, A. R., M. B. Bazdar, T. K. Sarkar, and R. F. Harrington, *AWAS for Windows Version 2.0: Analysis of Wire Antennas and Scatterers, Software and User'S Manual,* Artech House, 2002, ISBN: 1-58053-488-0.
8. ITU-R, P.1411-4, "Propagation data and prediction methods for the planning of short-range outdoor radio communication systems

and radio local area networks in the frequency range 300 MHz to 100 GHz," International Telecommunication Union, Geneva, 2001.

9. Chizhik, D. and J. Ling, "Propagation over clutter: Physical stochastic model," *IEEE Trans. on Antennas and Propagation*, Vol. 56, No. 4, 1071–1077, Apr. 2008.
10. Erceg, V, K. V. S. Hari, M. S. Smith, D. S. Baum, K. P. Sheikh, C. Tappenden, J. M. Costa, C. Bushue, A. Sarajedini, R. Schwartz, D. Branlund, T, Kaitz, and D. Trinkwon, "Channel models for fixed wireless applications," *Contribution IEEE P 802.16 3C-01/29r4, IEEE 802.16*, 2003.
11. Hata, M., "Empirical formula for propagation loss in land obile radio services," *IEEE Trans.Veh.Tech.*, Vol. 29, 317–325, 1980.
12. Soil dielectric properties (Dielectric materials and applications), NEC list, and website: pe2bz.philpem.me.uk/Comm/-%20Antenna/.../soildiel.htm.
13. Sarkar, T. K., S. Burintramart, N. Yilmazer, S. Hwang, Y. Zhang, A. De, and M. Salazar-Palma, "A discussion about some of the principles/practices of wireless communication under a Maxwellian framework," *IEEE Transactions on Antennas and Propagation*, Vol. 54, No. 12, 3727–3745, Dec. 2006.
14. Yarconi, N., N. Blaunstein, and D. Katz, "Link budget and radio coverage design for various multipath urban communication links," *RadioScience*, Vol. 42, RS2009, 1–15, 2007.
15. Erceg, V., S. Y. Tjandra, S. R. Parkoff, G. Ajay, K. Boris, A. A. Julius, and B. Renee, "An empirically based path loss model for wireless channels in suburban environments," *IEEE Journal on Selected Areas in Communs.*, Vol. 17, No. 7, 1205–1211, Jul. 1999.
16. Sarkar, T. K., "Near and far field antennas," Organized session on communications, *IEEE Conf. on Applied Electromagnetics*, 18–22, Kolkata, India, Dec. 2011.
17. Michaelides, C. P. and A. R. Nix, "Accurate high speed urban field strength predictions using a new hybrid statistical deterministic modeling technique," *54th Vehicular Technology Conf.*, Vol. 2, 1088–1092, Atlanta, NJ, USA, Oct. 7–11, 2001.
18. Milanovic, J., D. Rimac, and K. Bejuk, "Comparison of propagation models accuracy for wimax on 3.5 GHz," *ICECS 2007, 14th IEEE International Conf. on Electronics Circuits and Systems*, 111–114, Dec. 11–14, 2007.
19. Herring, K. T., J. W. Holloway, D. H. Staelin and D. W. Bliss, "Path loss characteristics of urban wireless channels," *IEEE Transactions on Antennas and Propagation*, Vol. 58, No. 1, 171–

177, Jan. 2010.

20. Sebastiao, D., D. Ladeina, M. Antunes, C. Oliveire, and L. M. Correia, "Estimation of base station exclusion zones," *VTC 2010 Fall*, 1–5, Ottawa, Sept. 6–9, 2010.
21. Baltzis, K. B., "A geometric method for computing the nodal distance distribution in mobile networks," *Progress In Electromagnetics Research*, Vol. 114, 159–175, 2011.
22. Gay-Fernandex, J. A., M. Garcia Sanchez, I. Cuinas, A. V. Alejos, J. G. Sanchez, and J. L. Miranda-Sierra, "Propagation analysis and deployment of a wireless sensor network in a forest," *Progress In Electromagnetics Research*, Vol. 106, 121–145, 2010.
23. Helhel, S., S. Ozen, and H. Goksu, "Investigation of GSM signal variation depending weather conditions," *Progress In Electromagnetics Research B*, Vol. 1, 147–157, 2008.
24. Phaiboon, S. and P. Phokharatkul, "Path loss prediction for low-rise buildings with image classification on 2-D aerial photographs," *Progress In Electromagnetics Research*, Vol. 95, 135–152, 2009.
25. Pu, S., J.-H. Wang, and Z. Zhang, "Estimation for small-scale fading characteristics of RF wireless link under railway communication environment using integrative modeling technique," *Progress In Electromagnetics Research*, Vol. 106, 395–417, 2010.
26. Tseng, H.-W., Y.-H. Lee, J.-Y. Lin, C.-Y. Lo, and Y.-G. Jan, "Performance analysis with coordination among base stations for next generation communication systems," *Progress In Electromagnetics Research B*, Vol. 36, 53–67, 2012.
27. Liu, Z.-Y. and L.-X. Guo, "A quasi three-dimensional ray tracing method based on the virtual source tree in urban microcellular environments," *Progress In Electromagnetics Research*, Vol. 118, 397–414, 2011.